

# Another new ring nematode, *Xenocriconemella andreae* sp. nov. (Nematoda, Criconematidae), from the Iberian Peninsula

Carolina Cantalapiedra-Navarrete<sup>1</sup>, Ilenia Clavero-Camacho<sup>1</sup>, Inmaculada Criado-Navarro<sup>1</sup>, Rosana Salazar-García<sup>1</sup>, Ana García-Velázquez<sup>1</sup>, Juan E. Palomares-Rius<sup>1</sup>, Pablo Castillo<sup>1</sup>, Antonio Archidona-Yuste<sup>1</sup>

<sup>1</sup> *Instituto de Agricultura Sostenible, Departamento de Protección de Cultivos, Avenida Menéndez Pidal s/n, 14004 Córdoba, Campus de Excelencia Internacional Agroalimentario, ceiA3, Spain*

<https://zoobank.org/E691CFAF-0825-43EA-8756-952C32174072>

Corresponding author: Antonio Archidona-Yuste (antonio.archidona@ias.csic.es)

Academic editor: A. Schmidt-Rhaesa ♦ Received 4 June 2024 ♦ Accepted 9 July 2024 ♦ Published 23 August 2024

## Abstract

Nematode surveys in natural environments in the Iberian Peninsula detected three unidentified *Xenocriconemella* populations that closely resembled the *X. macrodora*-species complex, but utilization of integrative taxonomy confirmed that they comprised a new taxon described in this paper as *X. andreae* sp. nov. Only females were detected in the new species (considered parthenogenetic) and delineated with a bare body (274–353 µm); lip region with two annuli, continuous with body delineation; second lip annulus enclosed by the first one. Flexible and thin stylet (88.0–99.0 µm), representing 30.4–47.8% of total body length. The excretory pore is positioned 2–3 annuli posterior to the level of stylet knobs, at 101.5 (87–107) µm from the lip region. Female genital tract: monodelphic, prodelphic, large, and representing 34.4–52.4% of the body length; vagina slightly ventrally curved. The anus is located at (6–9) annuli from the rear end. Tail short, conoid, and blunt round terminus. Ribosomal and mitochondrial markers (D2-D3 expansion domains of 28S, ITS, partial 18S rRNA, and COI), as well as molecular phylogenetic analyses of sequences, confirmed this new taxon, and it was clearly delineated from *X. macrodora* and species within the species complex (*X. costaricense*, *X. iberica*, *X. paraiberica*, and *X. pradense*).

## Key Words

COI, description, D2-D3, integrative taxonomy, ITS, 18S, morphometry

## Introduction

The ring nematode genus *Xenocriconemella* De Grisse & Loof, 1965 (De Grisse and Loof 1965) includes small ringed ectoparasite nematodes with a stylet ca. 40% of their body length. This species has become a topic of scientific attention in recent years. Particularly relevant is the novel incorporation of integrative taxonomy studies in deciphering populations within this genus (Archidona-Yuste et al. 2024; Peraza-Padilla et al. 2024). This unlocked the long-established assumption that *Xenocriconemella macrodora* (Taylor 1936; De Grisse and Loof 1965) was the unique valid species

within the genus. That is, recent integrative taxonomic studies added taxa within the genus *Xenocriconemella*, including the three new species described in the Iberian Peninsula (*X. iberica* Archidona-Yuste et al. 2024, *X. paraiberica* Archidona-Yuste et al. 2024, and *X. pradense* Archidona-Yuste et al. 2024) and the new one from Costa Rica (*X. costaricense* Peraza-Padilla et al. 2024). Undoubtedly, this has allowed us to support the validity and monophyly of this genus and has also confirmed the already reported strong association with forest and shrub ecosystems dominated mainly by *Quercus* trees (Bello et al. 1986; Gómez-Barcina et al. 1989; Escuer et al. 1999).

In Nematoda, and especially in plant-parasitic nematodes, it is quite typical that molecular differences are not manifested in variations in morphology among species (i.e., the occurrence of cryptic species complexes; Cantalapiedra-Navarrete et al. 2013; Archidona-Yuste et al. 2016, 2020; Cai et al. 2020; Clavero-Camacho et al. 2021). The integration and complementarity of different perspectives and methods of taxonomy is an imperative need for rigorous species delimitation within a cryptic complex (Proudlove and Wood 2003; Dayrat 2005; Fišer and Koselj 2022). Over the last 15 years, much research has been conducted on soil nematodes in this direction (particularly in plant-parasitic species; e.g., Gutiérrez-Gutiérrez et al. 2010; Barsi et al. 2017; Decraemer et al. 2024). The genus *Xenocriconemella* is a recent example where the transition from traditional to integrative taxonomy has unraveled a model cryptic complex of species (Archidona-Yuste et al. 2024). Indeed, molecular taxonomy together with in-depth morphological and morphometrical analyses defined the *X. macrodora*-species complex (*X. macrodora*, *X. iberica*, *X. paraiberica*, and *X. pradense*) from nematode populations widely distributed in the Iberian Peninsula (Archidona-Yuste et al. 2024). Furthermore, several studies have revealed a wide number of cryptic species complexes within a large functional variability of plant-parasitic nematodes in the Iberian Peninsula (e.g., Gutiérrez-Gutiérrez et al. 2010; Cantalapiedra-Navarrete et al. 2013; Archidona-Yuste et al. 2016, 2020; Cai et al. 2020; Archidona-Yuste et al. 2024; Decraemer et al. 2024; among others). Although it is well known that the Iberian Peninsula stands out as one of the most biodiverse regions on the planet (Myers et al. 2000), this great diversity detected in this area could also be due to the notable scientific effort in discovering the diversity of soil nematodes in this area developed in the last few years.

Here, to enhance soil nematode records and advance the understanding of taxonomy, morphology, and molecular data within the genus *Xenocriconemella*, we carried out a further sampling campaign on the *Quercus*-dominated natural areas of the Iberian Peninsula. In this nematode survey, we detected several unknown populations based on the available information (that is, morphological and molecular data) of *Xenocriconemella* species from the USA (Powers et al. 2021), Italy (Subbotin et al. 2005), Costa Rica (Peraza-Padilla et al. 2024), and the Iberian Peninsula (Archidona-Yuste et al. 2024). The original objective of this research was therefore to explore the

morphological-morphometrical and molecular diversity of these unresolved *Xenocriconemella* populations in the Iberian Peninsula genus and to compare them with the available morphometrical and molecular data by Archidona-Yuste et al. (2024). The key goals of this research were to (i) describe the three newly discovered Iberian Peninsula species both morphologically and morphometrically and compare them with other *Xenocriconemella* species in the *X. macrodora*-species complex; (ii) obtain molecular information about these *Xenocriconemella* populations using ribosomal (D2-D3 expansion domains of 28S rRNA, ITS region, partial 18S rRNA) and COI markers; and (iii) review the phylogenetic relationships of *Xenocriconemella andreae* sp. nov. within Criconemidae spp. and the *X. macrodora*-species complex.

## Materials and methods

### Nematode isolation and morphometrical characterization

Continuing the nematode surveys for deciphering the molecular and morphological diversity of *Xenocriconemella* isolates in the natural environments of the Iberian Peninsula started by Archidona-Yuste et al. (2024), three additional samples were collected in the autumn of 2023 containing an unidentified *Xenocriconemella* species (Table 1). Samples were taken from the rhizospheric soil of the selected plants and mixed to establish a single sample from each sample point. The soil samples were taken from a depth of 5 to 40 cm. Afterward, nematode specimens were isolated from a 500 cm<sup>3</sup> soil sub-sample using the centrifugal-flotation method (Coolen 1979).

Materials and methods used for light microscopy (LM) and morphometric studies followed the same protocols described by Archidona-Yuste et al. (2024) and other researchers (Seinhorst 1966; De Grisse, 1969). The following abbreviations (i.e., measurements and ratios) are used in the morphological descriptions, data analyses, and figures: **L** (total body length); **a** = body length/maximal body width; **b** = body length/pharyngeal length; **c** = body length/tail length; **c'** = tail length/body width at anus; **O** = distance between stylet base and orifice of dorsal pharyngeal gland as a percentage of stylet length; **R** = total number of body annuli; **R<sub>oes</sub>** = number of annuli in the pharyngeal region; **R<sub>ex</sub>** = number of annuli between the anterior end of the body and the excretory

**Table 1.** Host-plant species and localities of the analyzed populations of *Xenocriconemella andreae* sp. nov. inside the *Xenocriconemella macrodora* (Taylor, 1936) De Grisse and Loof 1965 species-complex from the Iberian Peninsula in this study.

Nematode species	Code	Host-plant species	Locality, province, Country	Abundance		NCBI Accessions		
				(Nem/500 cm <sup>3</sup> soil)	D2-D3	ITS	18S	COI
<i>Xenocriconemella andreae</i> sp. nov.	SIN03	<i>Pistacia lentiscus</i> L.	Linhó, Sintra, Portugal (type)	103	PP833567– PP833569	PP833563– PP833564	PP833577– PP833579	PP831172– PP831174
<i>Xenocriconemella andreae</i> sp. nov.	HUA03	<i>Quercus suber</i> L.	Aroche, Huelva, Spain	13	PP833570	-	-	PP831175– PP831176
<i>Xenocriconemella andreae</i> sp. nov.	LE002	<i>Castanea sativa</i> Mill.	Trabadelo, León, Spain	552	PP833571– PP833576	PP833565– PP833566	PP833580– PP833582	PP831177

pore; **Rst** = number of body annuli between labial disc and stylet knobs; **RV** = number of annuli between posterior end of body and vulva; **Rvan** = number of annuli between vulva and anus; **Ran** = number of annuli on tail; **V** = (distance from anterior end to vulva/body length)  $\times 100$ ; **VL/VB** = distance between vulva and posterior end of body divided by body width at vulva; **T** = (distance from cloacal aperture to anterior end of testis/body length)  $\times 100$  (Archidona-Yuste et al. 2023; 2024). The raw photographs were edited using Adobe Photoshop v. 22.5.2 (San Francisco, CA, USA).

### Molecular analyses

Total genomic DNA was extracted from single nematode specimens as previously described by Archidona-Yuste et al. (2023, 2024). As in previous studies, all four molecular markers for each *Xenocriconemella* isolate were obtained from the same PCR tube from a single individual without any exception.

Similarly to other studies, primers for ribosomal (D2-D3 expansion domains of 28S rRNA, internal transcribed pacer region (ITS) rRNA, and the partial 18S rRNA) and mitochondrial (COI) markers were the same as those specified in previous papers (De Ley et al. 1999; Subbotin et al. 2001; Hu et al. 2002; Derycke et al. 2005; Holterman et al. 2006). The PCR cycling conditions were also as described in previous papers (De Ley et al. 1999; Subbotin et al. 2005; Holterman et al. 2006; Powers et al. 2021). The PCR products were treated and sequenced at the Stab Vida sequencing facility (Caparica, Portugal) (see Archidona-Yuste et al. 2024 for details). The sequence chromatograms of all markers were analyzed with DNASTAR LASERGENE SeqMan v. 7.1.0. The species identity of the DNA sequences obtained in this study was confirmed by the basic local alignment search tool (BLAST) at the National Center for Biotechnology Information (NCBI) (Altschul et al. 1990). The accomplished sequences were delivered to the GenBank database under accession numbers specified on the phylogenetic trees and in Table 1.

### Species delineation analyses

We used two independent approaches to species delineation to resolve the species boundaries within the *X. macrodora* species complex, counting morphometric and molecular data.

First, we conducted a principal component analysis (PCA) to delimit species using morphometric data (Legendre and Legendre 2012). We established the species delimitation amongst the new *Xenocriconemella* populations found in the Iberian Peninsula and other species recently described within this genus, and we further evaluated the relationships between these new isolates and those previously designated within *Xenocriconemella*. PCA was constructed upon the following morphological

characters: L, stylet length, R, Rst, Roes, Rex, RV, Rvan, Ran, and the ratios a, b, c, V, VL/VB (Archidona-Yuste et al. 2024). For this analysis, we chose 25 *X. macrodora* s.l. populations previously characterized and recorded from numerous countries (Archidona-Yuste et al. 2024), as well as 28 Iberian populations previously studied under an integrative taxonomical approach, including 13 belonging to *X. iberica*, 12 belonging to *X. paraiberica*, 3 belonging to *X. pradense*, and 1 belonging to *X. costaricense* from Costa Rica (Archidona-Yuste et al. 2024; Peraza-Padilla et al. 2024). After data standardization (Zuur et al. 2010), the diagnostic character-data set was tested for collinearity using the values of the variance inflation factor (VIF) as recommended by Montgomery et al. (2012). PCA was carried out by means of the PCA function supplied in the software package ‘FactoMineR’ (Lê et al. 2008). All data analyses were performed with R version 4.2.2 (R Core Team 2022; <https://www.R-project.org>).

Species delimitation with molecular data and to compute intra- and inter-species disparity was performed by the P ID liberal and Rosenberg’s PAB value using the species delimitation plugin implemented in the software Geneious Prime v2022.1.1. (Geneious, Auckland, New Zealand) (Masters et al. 2011). Genetic distance was calculated based on intra- and interspecies molecular variations established by determining the ratio between the average genetic distance between specimens within a species and the average genetic distance between specimens belonging to sister species; if the ratio is less than 0.10, the probability of species identification is high (Masters et al. 2011). The P ID (liberal) value (Ross et al. 2008) means the likelihood that a correct species identification would be carried out using the closest genetic distance or placement on a tree (falling within or being sister to a monophyletic species clade). Taxa with a P ID (liberal)  $\geq 0.93$  were considered to be satisfactorily demarcated (Hamilton et al. 2014). Rosenberg’s P<sub>AB</sub> means the likelihood that the monophyly of a group of sequences is the result of random branching; significant values were  $<0.05$  (Rosenberg 2007).

### Phylogenetic analyses

Methods and software programs for aligning, sequence edition, and phylogenetic analyses were performed following the same procedures already specified in previous papers, including outgroup selection and tree visualization (Hall 1999; Ronquist and Huelsenbeck 2003; Darriba et al. 2012; Tan et al. 2015; Rambaut, 2018; Katoh et al. 2019; Ettongwe et al. 2020; Nguyen et al. 2022; Archidona-Yuste et al. 2024). The best-fit models for each marker were: the transitional model with invariable sites and a gamma-shaped distribution (TIM3 + I + G) for the D2-D3 expansion domains of 28S rRNA; the general time-reversible model with invariable sites and a gamma-shaped distribution (GTR + I + G) for ITS and the partial 18S rRNA gene; and the 3-parameter model with invariable sites and a gamma-shaped distribution (TPM3uf + I + G) for the COI gene.

## Results

Low to moderate densities (312, 13, -552 nematodes/500 cm<sup>3</sup> of soil) of the currently characterized isolates of *Xenocriconemella* were determined in the soil samples collected from the rhizosphere of mastic tree, cork oak, and chestnut Linhó, Sintra region, Portugal, Aroche, Huelva province, Spain, and Trabadelo, Leon province, Spain, respectively. Comprehensive morphological, morphometric, and molecular data about this species are supplied below, confirming its identification as a new taxon within the *Xenocriconemella macrodora*-species complex.

### Species delineation using morphometry

Our PCA results showed a wide intraspecific variation amongst the specimens of *Xenocriconemella* spp., especially for *X. iberica* and *X. paraiberica*, based on the wide morphometric variation in the following features: R, Rv, Roes, Rst, Rex, Stylet, V, and (VL/VB), confirming that previously described by Archidona-Yuste et al. (2024) (Fig. 1). As anticipated, we confirmed the high morphological variation displayed by *X. macrodora* (Archidona-Yuste et al. 2024). PCA clearly distinguished between almost all the individuals of *X. andreae* sp. nov., *X. pradense*, and *X. costaricense*, as well as those identified within *X. iberica* and *X. paraiberica*. However, this spatial separation occurred to a lower degree between *X. pradense* and *X. iberica*, where some individuals were found close to each other (Fig. 1). This species segregation was mostly observed along the first and second dimensions (Dim 1 and Dim2; 38.57 and 21.9% of the total variance, respectively). Dim1 was largely dominated by R, Rv, Roes, Rst, Rex, stylet length, and VL/VB (Fig. 1). On the other hand, Dim2 was mainly dominated by the Rvan and c ratio, thereby relating this dimension to the posterior part of the nematode. Except in specific cases, the delimitation of species boundaries provided by the PCA occurs through a linear combination of multiple diagnostic characters (Archidona-Yuste et al. 2016, 2024). Thus, we detected that species separations were mainly based on a combination of the following diagnostic characters: R, Roes, Rst, Rex, Rv, Rvan, c ratio, and stylet length. More explicitly, individuals with higher values in R, Rv, Roes, Rst, Rex, and Rv and longer stylet length were located on the right (i.e., *X. pradense* and *X. costaricense*), and those with lower values for these characters were located on the left side along Dim1 (i.e., *X. paraiberica* and *X. andreae* sp. nov.). Likewise, specimens with higher values of Rvan and c ratio (that is, longer length in the posterior part of the body) were located at the top (i.e., *X. costaricense* and *X. andreae* sp. nov.), and those with lower values for these characters were located at the bottom side along the Dim2 (i.e., *X. pradense*). Ultimately, we could conclude that Roes, Rst, Rex, and Rv were the most useful morphometrics for separating species within this cryptic complex in the genus *Xenocriconemella*. However, most of the specimens of *X. iberica* and

*X. paraiberica* were located overlying each other, given their similar values for traits associated with Dim 1 and Dim2 (Fig. 1). Thus, we confirmed that both species are strictly related morphologically. Additionally, we found an analogous arrangement for individuals (i.e., mean values of isolates) of *X. macrodora* as described by Archidona-Yuste et al. (2024). Definitively, our data confirmed the idea that these already described species (i.e., *X. iberica*, *X. paraiberica*, and *X. pradense*) encompass a model complex of cryptic species (i.e., the *X. macrodora* species complex). However, PCA allowed us to separate the new taxa *X. andreae* sp. nov. and the already described species (*X. costaricense*) from this species cryptic complex.

### Species delineation using ribosomal and mitochondrial DNA

Species delineation using ribosomal and mitochondrial markers proved that *X. andreae* sp. nov., *X. iberica*, *X. paraiberica*, *X. pradense*, and *X. costaricense* were undoubtedly distinguished among them, as were *X. macrodora* from the USA and Italy. The ratio between intra- and inter-species molecular variation for the D2–D3 expansion domains of 28S rRNA and the ITS region of all four Iberian Peninsula species was very low (0.01–0.08). In contrast, COI variation was higher in *X. macrodora* (0.33), followed by *X. iberica* (0.18), *X. paraiberica* (0.18), *X. andreae* sp. nov. (0.15), *X. pradense* (0.09), and *X. costaricense* (0.03), confirming that COI is more diversified in the USA than in the Iberian Peninsula and Costa Rica populations (Table 2). However, for all five species, the D2–D3 expansion domains of 28S rRNA and ITS genes undoubtedly displayed intra- and inter-species molecular variation (Table 2), signifying that the likelihood of species separation with these loci was high (Ross et al. 2008). Similarly, the P ID (liberal) values for all six species and loci were  $> 0.93$  (the probability for P ID (liberal) to be considered adequately delimited in the species delimitation is  $P \geq 0.93$ ), signifying that the six *Xenocriconemella* species can be adequately separated (Ross et al. 2008; Hamilton et al. 2014). The P ID (liberal) value (Ross et al. 2008) reveals the likelihood that a precise species identification would be completed using BLAST, the closest genetic distance, or placement on a tree. Species with a P ID (liberal)  $\geq 0.93$  were considered to be adequately delimited (Hamilton et al. 2014). Additionally, all clades were well-supported ( $PP = 1.00$ ) in the phylogenetic trees for the three loci, and Rosenberg's PAB values also supported the monophyly (Rosenberg's significant values =  $P < 0.05$ ) of the six species distinctly (Rosenberg 2007).

### Ribosomal and mitochondrial DNA characterization

*Xenocriconemella andreae* sp. nov. was molecularly characterized by the sequences of three ribosomal genes, D2–D3 expansion domains of 28S rRNA, ITS rRNA,

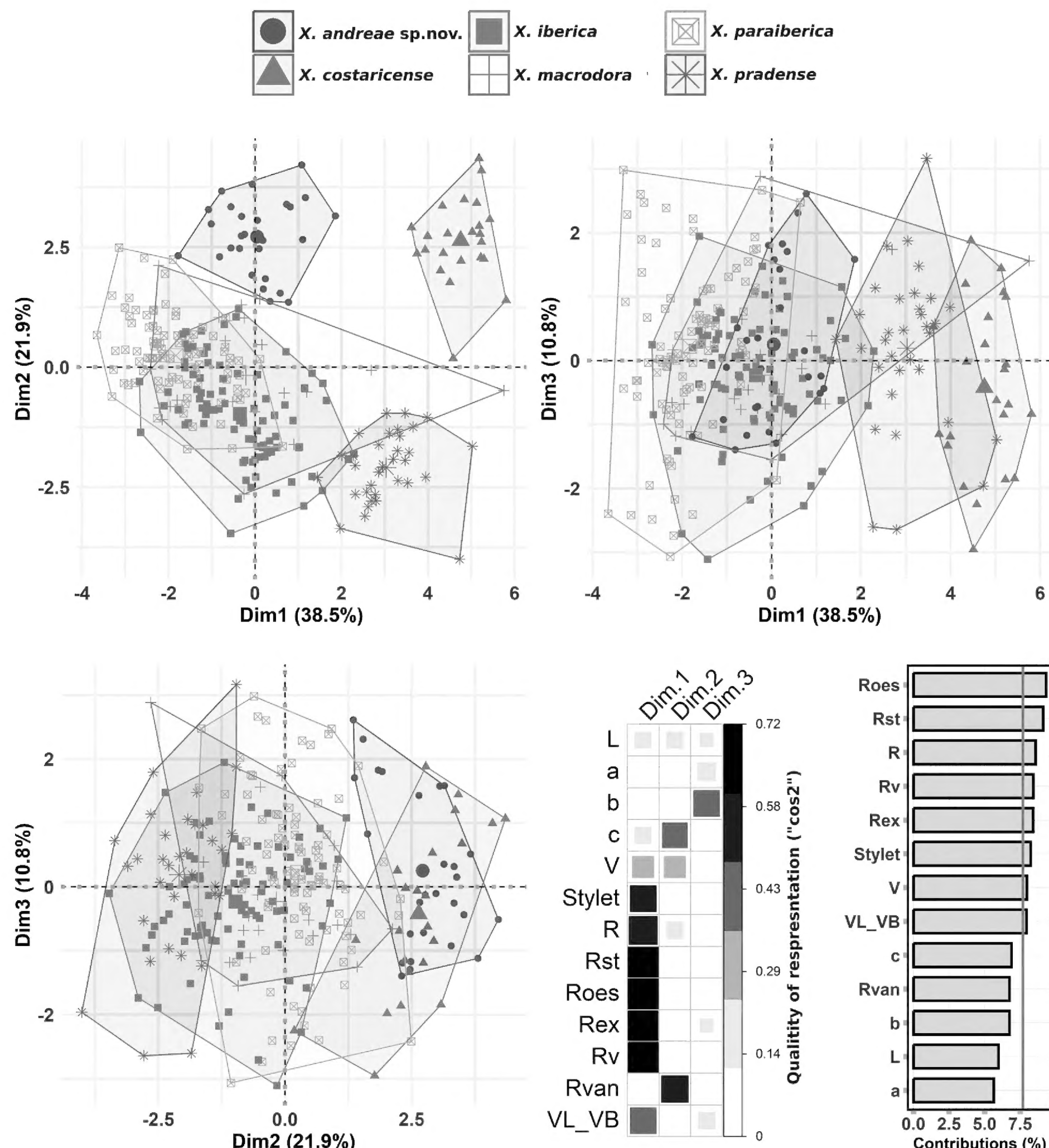


**Figure 1.** Principal component of the *Xenocriconemella macrodora* species complex. Projections of species on the plane of dimensions 1 and 2, 1 and 3, and 2 and 3. Correlation plot between dimensions and qualities of representation of the morphometric characters (“square cosine” ( $\cos^2$ )). Barplot showing the standardized contribution (%) of morphometric variables for the three dimensions retained by the PCA (only dimensions with sum of squares (SS) loadings  $> 1$  were extracted). A reference soil (red) line is also shown on the barplot. This reference line corresponds to the expected value if the contribution were uniform. For a given dimension, any row or column with a contribution above the reference line could be considered important in contributing to the dimension.

and partial 18S rRNA, and the mitochondrial gene COI. The amplification of these regions yielded single fragments of approximately 800, 800, 1600, and 400 bp, respectively, based on gel electrophoresis. Ten D2-D3 expansion domains of 28S rRNA sequences from 676 to 714 bp (PP833567–PP833576), four ITS rRNA sequences from 677 to 830 bp (PP833563–PP833566), six

18S rRNA sequences from 1681 to 1708 bp (PP833577–PP833582), and six COI sequences from 368 to 385 bp (PP831172–PP831177) were generated for this new species. Intraspecific sequence variations in ribosomal and mitochondrial markers were low in D2-D3 expansion domains of 28S rRNA (99.5–100.0%, 1–3 bp and 0 indel), in the ITS region (99.1–100.0%, 0–6 bp and 0–3 indels),

**Table 2.** Parameters evaluating *Xenocriconemella macrodora* species-complex delimitation based on two rRNA genes (D2-D3 expansion segments of the 28S rRNA, ITS) and one mtDNA barcoding locus, COI, for six *Xenocriconemella* species of the complex.

Species	Gene	Intra/Inter <sup>a</sup>	P ID (Liberal) <sup>b</sup>	Clade Support <sup>c</sup>	Rosenberg's P <sub>AB</sub> <sup>d</sup>
<i>Xenocriconemella macrodora</i>	D2-D3	-	-	-	-
	ITS	-	-	-	-
	COI	0.33	<b>0.97 (0.94, 0.99)</b> <sup>e</sup>	<b>1.00</b>	<b>1.2 × 10<sup>-31</sup></b>
<i>Xenocriconemella andreae</i> sp. nov.	D2-D3	0.08	<b>0.98 (0.93, 1.0)</b>	<b>1.00</b>	<b>5.6 × 10<sup>-7</sup></b>
	ITS	0.04	<b>0.97 (0.86, 1.0)</b>	<b>1.00</b>	<b>1.1 × 10<sup>-3</sup></b>
	COI	0.15	<b>0.96 (0.86, 1.0)</b>	<b>1.00</b>	<b>1.1 × 10<sup>-9</sup></b>
<i>Xenocriconemella iberica</i>	D2-D3	0.04	<b>0.98 (0.87, 1.0)</b>	<b>1.00</b>	<b>9.7 × 10<sup>-5</sup></b>
	ITS	0.02	<b>0.98 (0.87, 1.0)</b>	<b>1.00</b>	<b>4.1 × 10<sup>-3</sup></b>
	COI	0.18	<b>0.98 (0.95, 1.0)</b>	<b>1.00</b>	<b>1.1 × 10<sup>-9</sup></b>
<i>Xenocriconemella paraiberica</i>	D2-D3	0.05	<b>0.97 (0.87, 1.0)</b>	<b>1.00</b>	<b>1.1 × 10<sup>-3</sup></b>
	ITS	0.03	<b>0.97 (0.86, 1.0)</b>	<b>1.00</b>	<b>1.1 × 10<sup>-3</sup></b>
	COI	0.18	<b>0.98 (0.95, 1.0)</b>	<b>1.00</b>	<b>4.9 × 10<sup>-7</sup></b>
<i>Xenocriconemella pradense</i>	D2-D3	0.03	<b>0.98 (0.87, 1.0)</b>	<b>1.00</b>	<b>0.04</b>
	ITS	0.01	<b>0.98 (0.87, 1.0)</b>	<b>1.00</b>	<b>4.1 × 10<sup>-3</sup></b>
	COI	0.09	<b>0.98 (0.93, 1.0)</b>	<b>1.00</b>	<b>0.00</b>
<i>Xenocriconemella costaricense</i>	D2-D3	0.04	<b>0.97 (0.86, 1.0)</b>	<b>1.00</b>	<b>1.1 × 10<sup>-3</sup></b>
	ITS	0.02	<b>0.97 (0.82, 1.0)</b>	<b>1.00</b>	<b>4.9 × 10<sup>-3</sup></b>
	COI	0.03	<b>0.97 (0.86, 1.0)</b>	<b>1.00</b>	<b>4.9 × 10<sup>-7</sup></b>

<sup>a</sup> Intra-species variation relative to inter-species variation. <sup>b</sup> The P ID (liberal) value represents the probability (with the 95% confidence interval) for making a correct identification of an unknown specimen of the focal species using DNA barcoding (closest genetic distance). P ID (liberal) values  $\geq 0.93$  were considered to be significantly delimited (Hamilton et al. 2014). Numbers in bold represent significant values. <sup>c</sup> Clade support: posterior probabilities from Bayesian trees. <sup>d</sup> Rosenberg's P<sub>AB</sub> value is the probability that the monophyly of a group of sequences is the result of random branching; Rosenberg's significant values = P < 0.05. <sup>e</sup> Significant results are indicated in bold. (-) Not obtained or performed because only a single sequence of D2-D3 or ITS for this species is available in NCBI.

in 18S rRNA (99.8–100.0%, 0–3 bp and 0 indel), and in COI (97.8–100.0%, 0–8 bp and 0–1 indel). D2-D3 expansion domains of 28S rRNA of *X. andreae* sp. nov. (PP833567–PP833576) were 95.0–94.6% similar (differing by 33–41 bp, 2–4 indels) to *X. paraiberica* from Spain (OR880152–OR880200), 93.3–93.5% similar (differing by 33–44 bp, 0 indels) to *X. costaricense* from Costa Rica (PP209388–PP209391), 92.3–92.7% similar (differing by 49–50 bp, 3 indels) to *X. iberica* from Spain and Portugal (OR880112–OR880149), 91.0–91.3% similar (differing by 58 bp, 1 indel) to *X. pradense* from Spain (OR880203–OR880217), and 91.4–91.2% similar (differing by 47–48 bp, 1 indel) to *X. macrodora* from Italy (AY780960). ITS of *X. andreae* sp. nov. (PP833563–PP833566) was 82.7% similar (differing by 138 bp, 51 indels) to *X. costaricense* from Costa Rica (PP209397, PP209398), 80.9–81.1% similar (differing by 165–167 bp, 102–103 indels) to *X. paraiberica* from Spain (OR878338–OR878349), 80.8% similar (differing by 161 bp, 49 indels) to *X. pradense* (OR878350), 79.5% similar (differing by 173–174 bp, 76–77 indels) to *X. iberica* (OR878332–OR878336), and 78.2–78.6% similar (differing by 64–65 bp, 33–34 indels) to *X. macrodora* from USA (JQ708139), but with a low coverage (50–59%). Partial 18S rRNA of *X. andreae* sp. nov. (PP833577–PP833582) was 98.8% similar (differing by 20 bp, 5 indels) to *X. paraiberica* (OR878358), 98.6–98.7% similar (differing by 23–24 bp, 3–4 indels) to *X. macrodora* (MF094906, MF094973, MF095001), 98.2–98.5% similar (differing by 25–30 bp, 3 indels) to *X. costaricense* (PP209396), 97.9–98.1% similar (differing by 32–35 bp, 5 indels) to *X. pradense* (OR878360–OR878361), and 97.8% similar (differing by 37 bp, 5 indels) to *X. iberica* (OR878356). Finally, COI of *X. andreae* sp. nov. (PP831172–PP831177) was 92.5–93.4% similar (differing by 23–27 bp, 0–1 indel) to *X. iberica* from Spain and Portugal (OR885936–OR885976), 90.3–92.0% sim-

ilar (differing by 28–36 bp, 0–1 indel) to *X. paraiberica* from Spain (OR885983–OR886017), 89.1% similar (differing by 41–36 bp, 1 indel) to *X. costaricense* from Costa Rica (PP210897–PP210900), 89.0–91.7% similar (differing by 37–46 bp, 1 indel) to *X. macrodora* from USA (MF770894–MF770950, MN711386–MN711444), and 89.8–90.2% similar (differing by 31–32 bp, 1 indel) to *X. pradense* from Spain (OR886020–OR886029).

## Phylogenetic analysis

Phylogenetic analysis among *Xenocriconemella* species, based on the D2–D3 expansion domains of 28S, ITS, the partial 18S rRNA, and the partial COI mtDNA gene sequences, was carried out using BI (Figs 2, 3, 4, 5, respectively). The phylogenetic trees created with the ribosomal and mitochondrial DNA markers included 78, 61, 94, and 171 sequences, and their alignment had 702, 728, 1694, and 360 characters, respectively. The Bayesian 50% majority rule consensus tree inferred from the D2-D3 expansion domains of the 28S rRNA alignment is given in Fig. 2. For this ribosomal marker, all six species belonging to the genus *Xenocriconemella* clustered together in a well-supported clade (PP = 1.00), clearly separated from all other genera within Criconematidae (Fig. 2). The *Xenocriconemella* clade was subdivided into four subclades; one of them (PP = 1.00) comprises all the sequences for *X. andreae* sp. nov. (PP833567–PP833576), followed by another one (PP = 0.96) including *X. paraiberica* (OR880152–OR880202) and *X. costaricense* (PP209388–PP209391), the third one (PP = 0.99) comprises *X. pradense* (OR880203–OR880218) and the single sequence for *X. macrodora* from Italy (AY780960), and the fourth subclades include *X. iberica* (OR880107–OR880151).

## 28S

### Criconematidae spp.

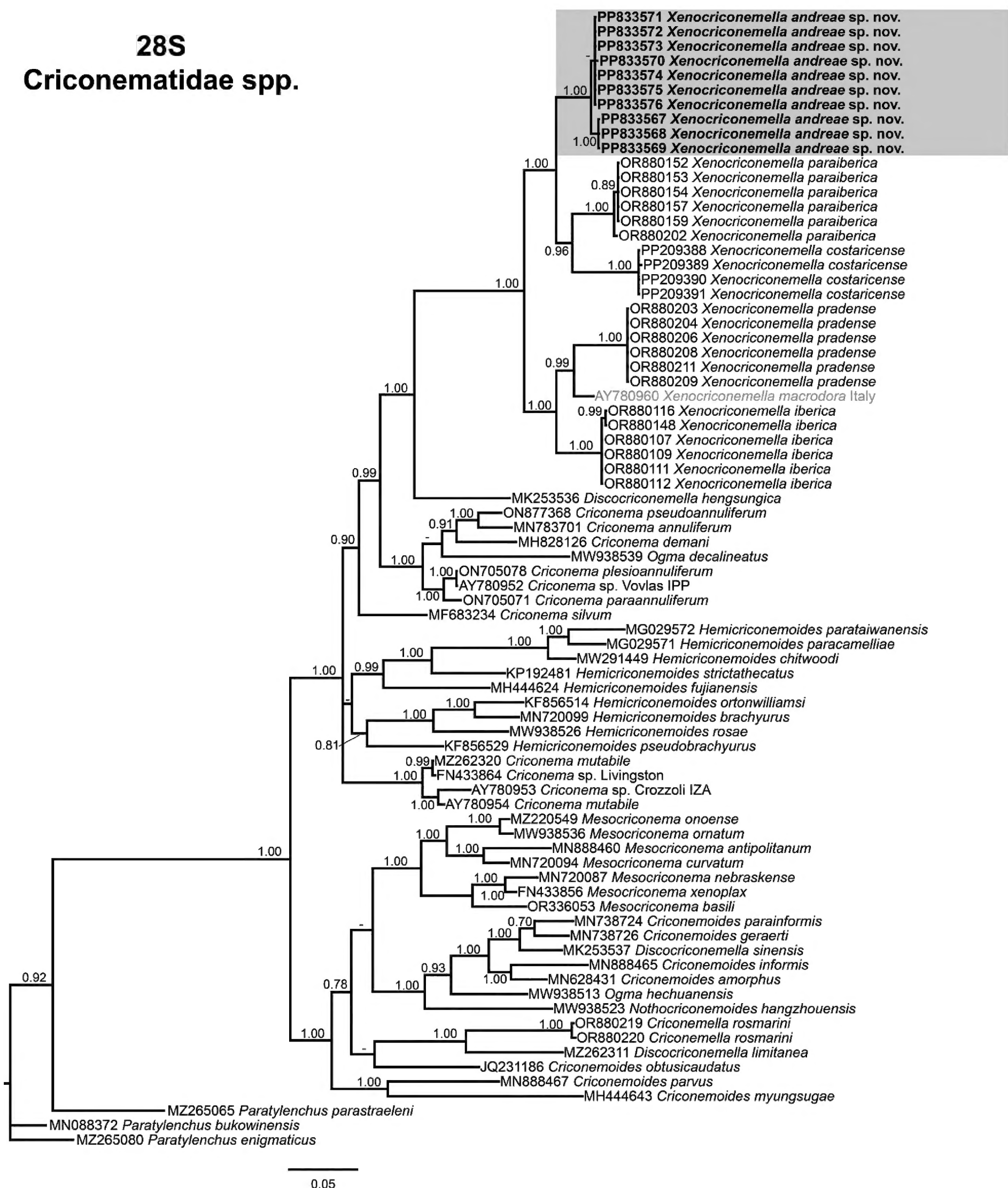
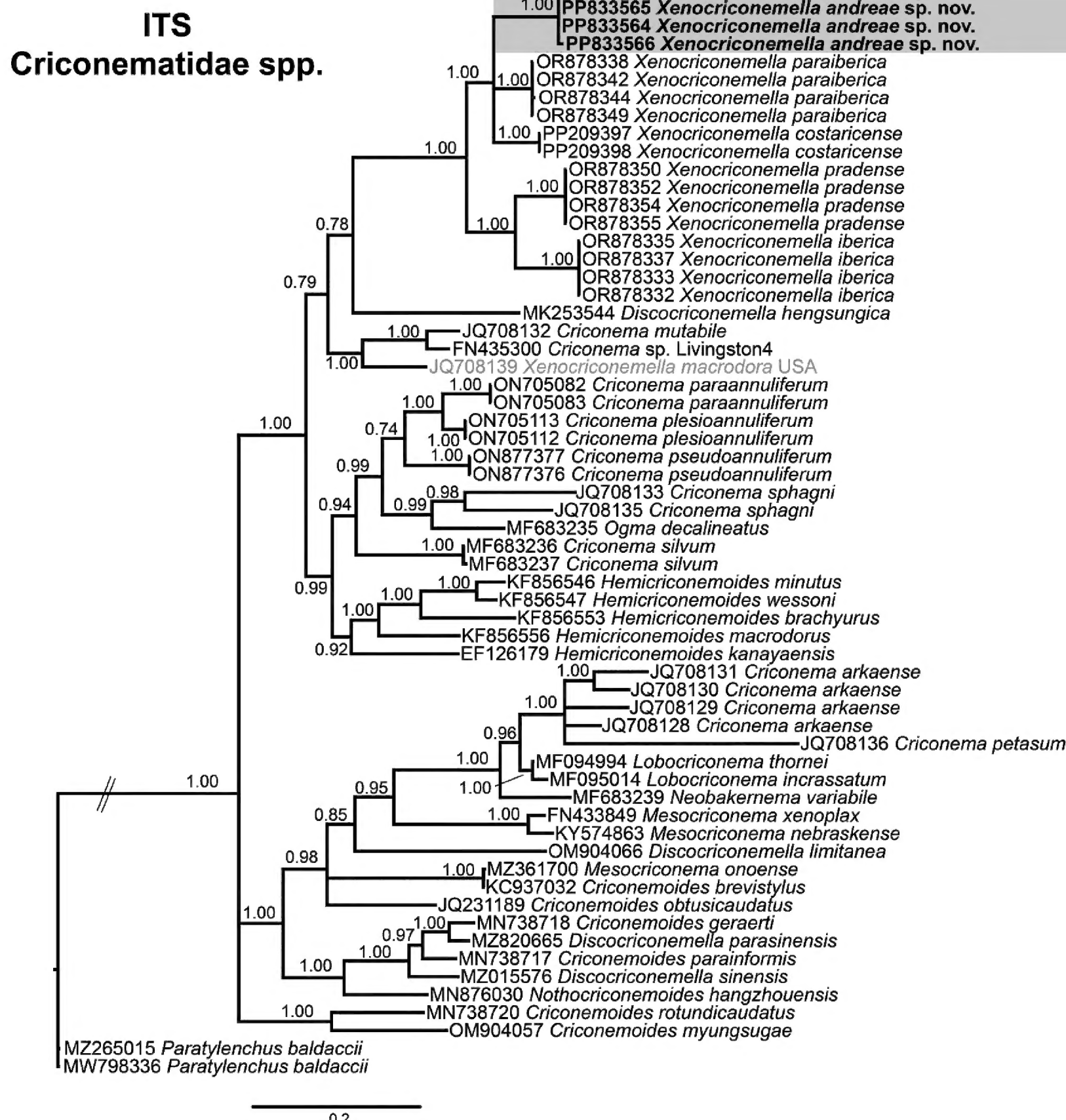


**Figure 2.** Phylogenetic relationships of *Xenocriconemella andreae* sp. nov. with Criconematidae spp. Bayesian 50% majority rule consensus tree as inferred from D2 and D3 expansion domains of 28S rRNA sequence alignment under the TIM3 + I + G model ( $-\ln L = 8665.6142$ ; AIC = 17655.228420; freqA = 0.1888; freqC = 0.2391; freqG = 0.3304; freqT = 0.2418; R(a) = 0.4795; R(b) = 1.6113; R(c) = 1.0000; R(d) = 0.4795; R(e) = 4.0922; R(f) = 1.0000; Pinva = 0.4170; and Shape = 0.9390). Posterior probabilities greater than 0.70 are given for appropriate classes. The newly obtained sequences in this study are shown in bold, and colored boxes indicate the clade association of the new species. Scale bar: expected changes per site.

In the ITS region tree (Fig. 3), phylogenetic relationships showed all *Xenocriconemella* species, except for *X. macrodora* from the USA (JQ708139), within a well-supported clade (PP = 1.00), undoubtedly separated

from all other genera of Criconematidae. This clade was subdivided into two subclades, one of them (PP = 1.00), comprising all the sequences for *X. andreae* sp. nov. (PP833563–PP833566), *X. paraiberica* (OR878338–



## 18S

### Criconematidae spp.



**Figure 4.** Phylogenetic relationships of *Xenocriconemella andreae* sp. nov. with Criconematidae spp. Bayesian 50% majority rule consensus tree as inferred from 18S rRNA sequence alignment under the GTR + I + G model ( $-\ln L = 7859.2560$ ;  $AIC = 16114.51198$ ;  $\text{freqA} = 0.2451$ ;  $\text{freqC} = 0.2388$ ;  $\text{freqG} = 0.2784$ ;  $\text{freqT} = 0.2378$ ;  $R(a) = 1.4017$ ;  $R(b) = 2.0249$ ;  $R(c) = 1.0058$ ;  $R(d) = 0.6630$ ;  $R(e) = 5.7196$ ;  $R(f) = 1.0000$ ;  $\text{Pinva} = 0.6610$ ; and  $\text{Shape} = 0.5740$ ). Posterior probabilities greater than 0.70 are given for appropriate classes. The newly obtained sequences in this study are shown in bold, and colored boxes indicate the clade association of the new species. Scale bar: expected changes per site.



**Figure 5.** Phylogenetic relationships of *Xenocriconemella andreae* sp. nov. with other *Xenocriconemella* spp. Bayesian 50% majority-rule consensus trees as inferred from cytochrome c oxidase subunit I (COI) mtDNA gene sequence alignments under the TPM3uf + I + G model ( $-\ln L = 2464.7614$ ; AIC = 5639.5228; freqA = 0.3727; freqC = 0.0511; freqG = 0.0810; freqT = 0.4953; R(a) = 1.7003; R(b) = 9.5660; R(c) = 1.0000; R(d) = 1.7003; R(e) = 9.5660; R(f) = 1.0000; Pinva = 0.3460; and Shape = 0.4040). Posterior probabilities greater than 0.70 are given for appropriate classes. The newly obtained sequences in this study are shown in bold, and colored boxes indicate the clade association of the new species. Scale bar = expected changes per site.

but the phylogenetic relationship with them was not well resolved (Fig. 5). Sequences from *X. macrodora* from the USA appeared together in a well-supported (PP = 1.00) subclade.

## Taxonomy

**Phylum: Nematoda Rudolphi, 1808**

**Class: Chromadorea Inglis, 1983**

**Order: Rhabditida Chitwood, 1933**

**Suborder: Tylenchina Chitwood, 1950**

**Superfamily: Criconematoidea Khan & Ahmad, 1975**

**Family: Criconematidae Taylor, 1936**

**Genus: *Xenocriconemella* De Grisse & Loof, 1965**

***Xenocriconemella andreae* sp. nov.**

<https://zoobank.org/1A7BEE7F-3C2A-4E9F-8031-F5AD3C1300E2>

**Description. Females.** Body ventrally arcuate to straight, slightly narrowing anteriorly and posteriorly. Body annuli smooth and retrorse 2.6 (2.5–3.0)  $\mu\text{m}$  wide, without anastomosis (Fig. 6). Lip region with two annuli, not offset, not separated from body contour; first lip annulus par-

tially covering the second lip annulus (Fig. 6); second lip annulus retrorse and slightly wider than first annulus 9.1 (8.0–10.0)  $\mu\text{m}$  wide. Stylet thin, long, and flexible (Figs 6, 7, Table 3), occupying 31 (27.2–35.0)% of the body length, with short basal portion 7.2 (7.0–8.0)  $\mu\text{m}$  long and knobs slightly rounded 5.1 (5.0–6.0)  $\mu\text{m}$  wide. Pharynx typical criconematoid, with a cylindroid procorpus widening to a large muscular oval median bulb containing well-developed valves (8.0–9.5  $\mu\text{m}$  long), istmus slender, and amalgamated with basal bulb. Excretory pore located from two to three annuli posterior to level of stylet knobs, at 102 (87.0–107.0)  $\mu\text{m}$  from anterior end. Nerve ring located at the level of istmus, 116 (103–124)  $\mu\text{m}$  from the anterior end. Vagina ventrally curved (14.0–17.0  $\mu\text{m}$  long). Female genital tract monodelphic, prodelphic, outstretched, and occupying 43 (34.4–52.4)% of the body length; spermatheca almost hemispherical (11.0–14.0  $\times$  12.5–18.0)  $\mu\text{m}$ , sperm absent. Anus located at 7.7 (6–9) annuli from the terminus. Tail short, conoid, and bluntly rounded terminus.

**Males.** Not found.

**Juveniles.** Body similar to females, including tail shape, but shorter. Edge of body annuli without appendages, marked with delicate irregular punctations.

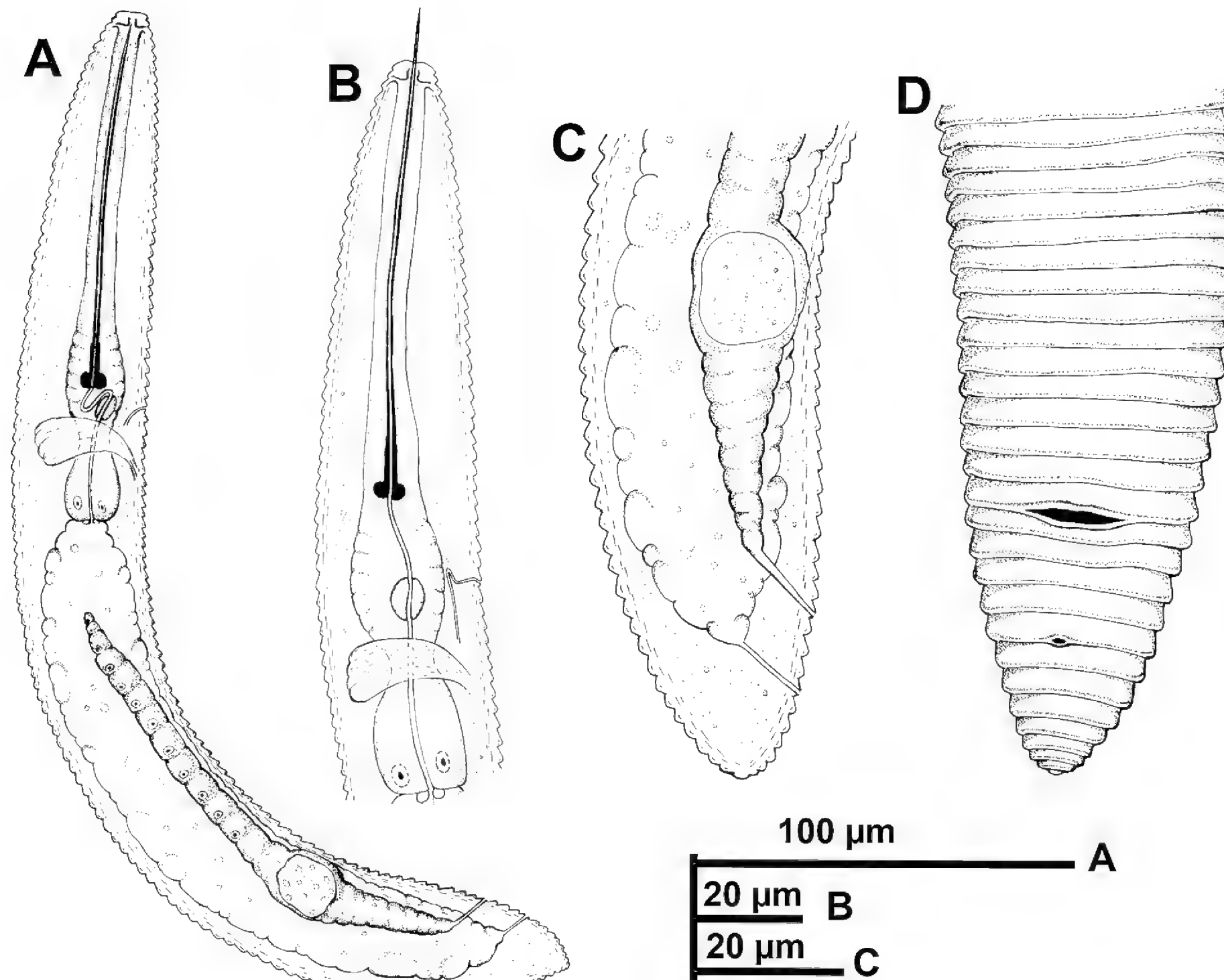


**Figure 6.** *Xenocriconemella andreae* sp. nov. (drawings). **A.** Entire female; **B.** Female anterior region; **C, D.** Detail of female posterior region showing vulva and anus.

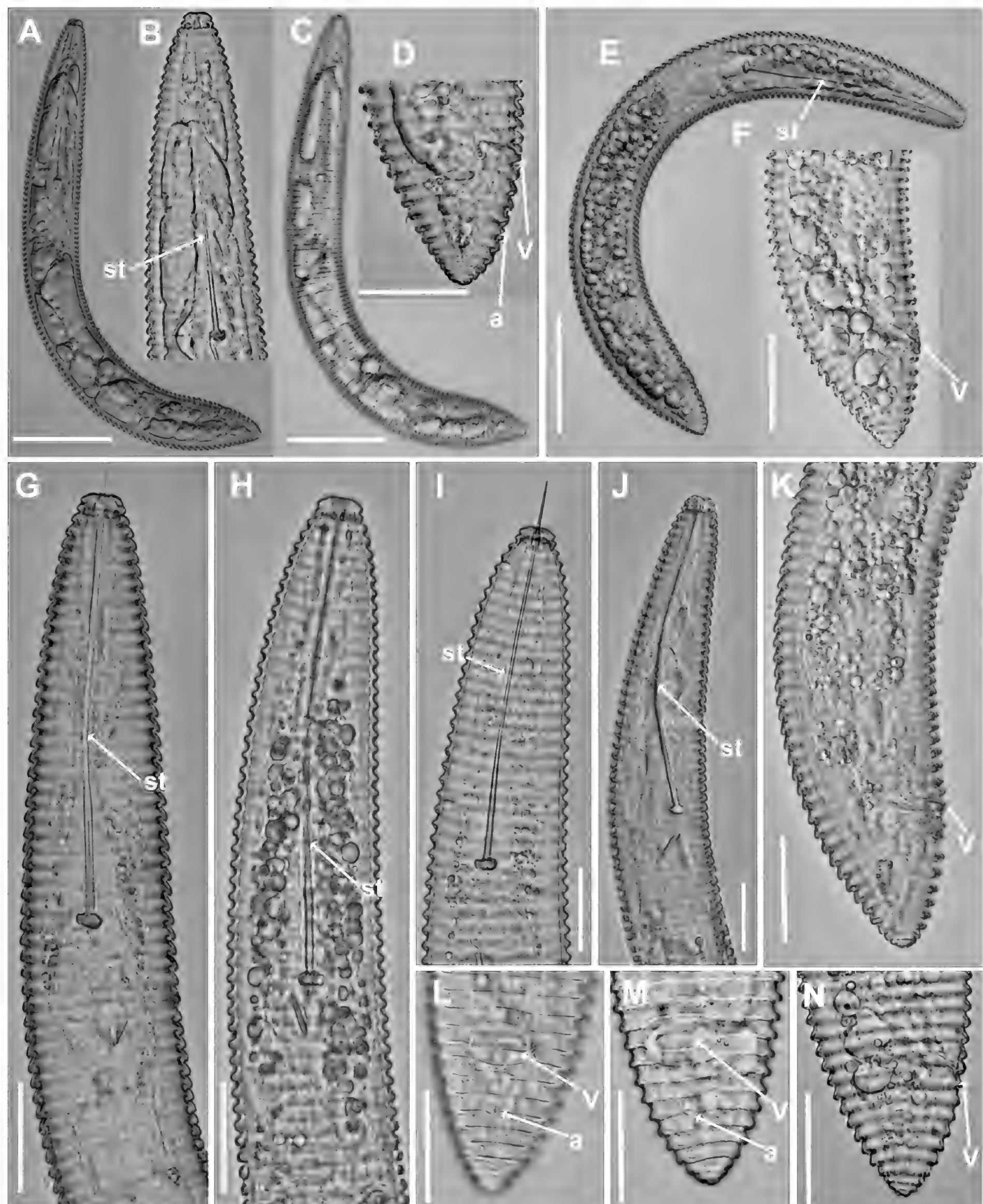


**Figure 7.** Light micrographs of *Xenocriconemella andreae* sp. nov. **A, E.** Entire female; **C.** Entire female showing body annuli without anastomosis; **B, G–J.** Female anterior body region showing stylet (arrowed); **D, F, K–N.** Vulval region showing vulva and anus (arrowed). Abbreviations: a = anus; st = stylet; V = vulva. Scale bars: 50  $\mu$ m (A, C, E); 20  $\mu$ m (B, D, F–N).

**Diagnosis and relationships.** *Xenocriconemella andreae* sp. nov. is characterized by the following measurements and ratios: a short-sized female body 307 (274–353)  $\mu$ m, a long and flexible stylet = 94.6 (88.0–99.0)  $\mu$ m long,

V = 92 (90.2–92.5), a = 10.2 (8.4–12.2), b = 2.3 (2.1–2.6), c = 26.3 (21.9–32.5), c' = 0.7 (0.6–0.8), R = 113 (105–119), RV = 10.7 (9–12), Ran = 7.7 (6–9), VL/VB = 1.0 (0.8–1.1). Morphologically and morphometrically,

**Table 3.** Morphometrics of *Xenocriconemella andreae* sp. nov. from the rhizosphere of mastic tree, cork oak, and chestnut from Linhó, Sintra region, Portugal; Aroche, Huelva province, Spain; and Trabadelo, León province, Spain<sup>1</sup>.

Character <sup>1</sup>	Portugal		Spain	
	Holotype	Paratype Females	Aroche, Huelva province	Trabadelo, León province
n	1	20	3	4
L	302	307.2 ± 21.0 (274–353)	331.3 ± 24.7 (303–348)	341.3 ± 12.9 (323–353)
R	114	112.5 ± 4.1 (105–119)	110.7 ± 2.9 (109–114)	114.3 ± 2.9 (111–118)
Rst	35	36.0 ± 2.4 (31–40)	34.7 ± 0.6 (34–35)	34.5 ± 1.3 (33–36)
Roes	47	47.7 ± 2.6 (42–52)	45.3 ± 1.2 (44–46)	46.0 ± 1.4 (45–48)
Rex	38	38.5 ± 2.6 (33–43)	37.0 ± 1.0 (36–38)	36.8 ± 1.0 (36–38)
RV	10	10.7 ± 0.8 (9–12)	12.3 ± 0.6 (12–13)	11.3 ± 1.0 (10–12)
Rvan	3	3.0 ± 0.0 (3–3)	3.0 ± 0.0 (3–3)	3.0 ± 0.0 (3–3)
Ran	7	7.7 ± 0.7 (6–9)	9.3 ± 0.6 (9–10)	8.3 ± 1.0 (7–9)
O	0.9	8.2 ± 0.4 (7.4–8.9)	7.6 ± 0.5 (7.4–8.2)	7.5 ± 0.5 (7.1–8.2)
A	8.9	10.2 ± 1.1 (8.4–12.2)	11.6 ± 0.6 (11.2–12.3)	11.5 ± 0.6 (10.7–11.9)
B	2.2	2.3 ± 0.1 (2.1–2.6)	2.5 ± 0.1 (2.4–2.5)	2.6 ± 0.1 (2.5–2.7)
C	22.4	26.3 ± 3.4 (21.9–32.5)	18.7 ± 0.8 (17.8–19.3)	20.2 ± 1.5 (18.7–22.3)
c'	0.6	0.7 ± 0.05 (0.6–0.8)	0.8 ± 0.03 (0.8–0.9)	0.8 ± 0.04 (0.7–0.9)
V	91.1	91.5 ± 0.7 (90.2–92.5)	90.8 ± 0.8 (90.2–91.7)	90.9 ± 0.7 (90.4–92.0)
VL/VB	0.9	1.0 ± 0.1 (0.8–1.1)	1.2 ± 0.06 (1.2–1.3)	1.1 ± 0.05 (1.1–1.2)
Stylet	95.0	94.6 ± 2.9 (88.0–99.0)	96.0 ± 1.7 (95.0–98.0)	96.3 ± 1.5 (95.0–98.0)
Pharynx	135	132.5 ± 5.1 (122–140)	133.3 ± 5.7 (127–138)	133.3 ± 6.1 (127–139)
Max. body width	34	30.5 ± 3.3 (24.0–37.0)	28.7 ± 2.1 (27.0–31.0)	29.8 ± 2.2 (28.0–33.0)
Anal body width	21	17.6 ± 1.9 (14.5–21.0)	20.8 ± 1.0 (20.0–22.0)	21.1 ± 1.7 (19.5–23.0)
Vulva to anus distance	14	12.7 ± 1.8 (10.0–16.0)	13.2 ± 1.0 (12.0–14.0)	13.3 ± 2.0 (11.5–16.0)
Tail	13.5	11.9 ± 1.5 (10.0–14.0)	17.7 ± 0.6 (17.0–18.0)	17.0 ± 1.8 (14.5–18.5)

<sup>1</sup>All measurements are in  $\mu\text{m}$  and in the form: mean ± s.d. (range).

*X. andreae* sp. nov. resembles members of the *X. macrodora*-species complex (including *X. macrodora*, *X. iberica*, *X. paraiberica*, *X. pradense*, and *X. costaricense*), from which it can be separated by several morphometric traits and ratios. From *X. macrodora*, it is almost undistinguishable but mainly differs by a slightly higher c ratio 26.3 (21.9–32.5) vs. 19.6 (12.8–25.3). From *X. iberica*, it is also almost undistinguishable, but differs by a slightly shorter tail length 11.9 (10.0–14.0)  $\mu\text{m}$  vs. 16.4 (11.0–24.5)  $\mu\text{m}$  and a slightly higher c ratio 26.3 (21.9–32.5) vs. 18.3 (12.1–27.3). From *X. paraiberica*, it is also almost undistinguishable, but mainly differs by a slightly longer stylet length 94.6 (88.0–99.0)  $\mu\text{m}$  vs. 89.6 (80.0–100.0)  $\mu\text{m}$ , a higher number of body annuli (R) 112.5 (105–119) vs. 104 (95–116), and a slightly higher c ratio 26.3 (21.9–32.5) vs. 20.2 (13.0–28.6). From *X. pradense*, it mainly differs by a slightly lower VL/VB ratio 1.0 (0.8–1.1) vs. 1.4 (1.1–1.5), a lower number of body annuli from vulva to posterior end (RV) 10.7 (9–12) vs. 16 (14–18), a slightly shorter tail length 11.9 (10.0–14.0)  $\mu\text{m}$  vs. 20.2 (15.5–25.0)  $\mu\text{m}$ , a higher c ratio 26.3 (21.9–32.5) vs. 16.6 (13.7–21.3), and a lower c' ratio 0.7 (0.6–0.8) vs. 0.9 (0.8–1.2). Finally, *X. andreae* sp. nov. clearly differs from *X. costaricense* by a shorter body length 307.2 (274–353)  $\mu\text{m}$  vs. 349 (276–404)  $\mu\text{m}$ , a shorter stylet length 94.6 (88.0–99.0)  $\mu\text{m}$  vs. 125 (113.0–133.0)  $\mu\text{m}$ , a slightly higher number of body annuli (R) 112.5 (105–119) vs. 124 (117–130), a slightly higher c ratio 26.3 (21.9–32.5) vs. 22.8 (16.0–28.8), and a slightly lower VL/VB ratio 1.0 (0.8–1.1) vs. 1.1 (0.9–1.3).

**Etymology.** The species epithet refers to the name of the daughter of the last author, Miss. Andrea Archidona Rosales, who helped to take the sample of the type population.

**Type host and locality.** The new species was recovered from the rhizosphere of a mastic tree (*Pistacia lentiscus* L.) at Linhó, Sintra region, Portugal (coordinates 38°46'07.78"N, 9°23'41.96"W). Additional specimens were detected from the rhizosphere of cork oak (*Quercus suber* L.) and chestnut (*Castanea sativa* Mill.) at Aroche, Huelva province, Spain (coordinates 37°54'13.06"N, 6°37'02.95"W), and Trabadelo, León province, Spain (coordinates 42°38'38.3"N, 6°52'14.0"W), respectively.

**Type material.** Holotype female and 16 female paratypes deposited at the nematode collection of the institute for sustainable agriculture (IAS) of the Spanish National Research Council (CSIC; collection nos. XEN-AND-01/XEN-AND-16), Córdoba, Spain; and two females at the USDA Nematode Collection (T-8065p).

## Discussion

Late studies based on integrative taxonomy on profuse *X. macrodora*-species complex populations from the Iberian Peninsula and a population from Costa Rica clearly demonstrate that the cosmopolitan species *X. macrodora* need to be considered a species complex including at least five species, *viz.* *X. iberica*, *X. macrodora*, *X. paraiberica*, *X. pradense*, and *X. costaricense*, and probably comprising additional new cryptic species all over the world (Archidona-Yuste et al. 2024; Peraza-Padilla et al. 2024). Because of their basic morphology and a wide morphometric range of populations all over the world (Archidona-Yuste et al. 2024), accurate species identification within the genus *Xenocriconemella* has only been possible after applying integrative taxonomical studies,

allowing to decipher the presence of cryptic species (Archidona-Yuste et al. 2024; Peraza-Padilla et al. 2024). The main goal here was to describe and identify morphologically and molecularly the three new populations of *Xenocriconemella* found in natural environments on the Iberian Peninsula, as well as clarify phylogenetic relationships within this genus. Our results corroborate that the three new *Xenocriconemella* populations studied here are morphologically and morphometrically related to the *X. macrodora*-species complex, except for some minor morphometric features. Nevertheless, all the molecular markers certainly delineated the three new Iberian Peninsula populations from all other species within this genus, confirming that they comprise a new valid species within the genus *Xenocriconemella*. These data provide a clear indication that the global biodiversity of this genus is much greater than previously suspected, as has been suggested recently by Archidona-Yuste et al. (2024) and Peraza-Padilla et al. (2024). Certainly, although more studies are required to confirm this assumption on a global scale, the present results indicate that additional new taxa can be detected within the widely reported populations of *X. macrodora* s.l. in those regions of the Iberian Peninsula where the species complex has been reported (Archidona-Yuste et al. 2024).

Ribosomal and mitochondrial markers (D2-D3 expansion domains of the 28S and ITS rRNA and the mtDNA gene COI) are again demonstrated to be important tools for the accurate identification of *Xenocriconemella* spp. and other Criconematidae (Subbotin et al. 2005; Etongwe et al. 2020; Powers et al. 2021; Nguyen et al. 2022; Archidona-Yuste et al. 2024). In our studies on the molecular diversity of *Xenocriconemella* spp. in the Iberian Peninsula, ribosomal markers looked like the best molecular tools for identifying *Xenocriconemella* species since they showed the lowest intraspecific variability. Phylogenetic analyses based on D2-D3, ITS, 18S, and COI genes using BI mostly clearly demonstrated the monophyly of the genus *Xenocriconemella*, were consistent with those given by previous phylogenetic analyses (Subbotin et al. 2005; Etongwe et al. 2020; Nguyen et al. 2022; Archidona-Yuste et al. 2024; Peraza-Padilla et al. 2024), and confirmed the validity of *Xenocriconemella* within Criconematidae. Our data also suggest that the 18S rRNA accession of *X. macrodora* from Portugal (MT229843, differing by 12 bp from *X. andreae* sp. nov.) was most likely misidentified as hypothesized by Archidona-Yuste et al. (2024). Unfortunately, no additional molecular data were available in GenBank from this population, and further studies will be needed to clarify this identification, linking morphological and molecular data through integrative taxonomy. Similarly, the high diversity (up to 25%, 101–115 bp and 40–45 indels) among ITS sequences of *Xenocriconemella* spp. from the Iberian Peninsula and Costa Rica with the sequence of *X. macrodora* from the USA (JQ708139) suggests a misidentification that should be confirmed with additional studies since no other molecular markers of this population are available (Cordero et al. 2012).

## Conclusions

This study expands our understanding of the biodiversity of the genus *Xenocriconemella* in the Iberian Peninsula. It also confirms the effectiveness of using an integrative approach that combines morphometric and morphological characteristics with the genotyping of rRNA and mtDNA markers for accurate species identification among *Xenocriconemella* species. Additionally, the study highlights the need for ongoing nematode surveys in natural habitats to uncover the uncharted biodiversity of this genus globally.

## Acknowledgements

This work was supported by the Consejería de Universidad, Investigación e Innovación-Junta de Andalucía, Qualifica Project (QUAL21\_023 IAS). A. Archidona-Yuste is funded by the Ramón y Cajal program (RYC2021-031108-I), and I. Criado-Navarro is funded by the Juan de la Cierva programs (JDC2022-048855-I), funded by MCIN/AEI/10.13039/501100011033 and UE “Next Generation EU/PRTR.” The authors thank Gracia Liébanas and María Rodríguez Santamaría for their help with sampling. In addition, the authors thank Jorge Martín Barbarroja (IAS-CSIC), Guillermo León-Ropero (IAS-CSIC), and Inmaculada Casero Godoy for their excellent technical assistance.

## References

- Altschul SF, Gish W, Miller W, Myers EW, Lipman DJ (1990) Basic local alignment search tool. *Journal of Molecular Biology* 215(3): 403–410. [https://doi.org/10.1016/S0022-2836\(05\)80360-2](https://doi.org/10.1016/S0022-2836(05)80360-2)
- Archidona-Yuste A, Navas-Cortes JA, Cantalapiedra-Navarrete C, Palomares-rius JE, Castillo P (2016) Cryptic diversity and species delimitation in the *Xiphinema americanum*-group complex (Nematoda, Longidoridae) as inferred from morphometrics and molecular markers. *Zoological Journal of the Linnean Society* 176(2): 231–265. <https://doi.org/10.1111/zoj.12316>
- Archidona-Yuste A, Cai R, Cantalapiedra-Navarrete C, Carreira JA, Rey A, Viñegla B, Liebanas G, Palomares-Rius JE, Castillo P (2020) Morphostatic speciation within the dagger nematode *Xiphinema hispanum*-complex species (Nematoda, Longidoridae). *Plants* 9(12): 1649. <https://doi.org/10.3390/plants9121649>
- Archidona-Yuste A, Palomares-Rius JE, Clavero-Camacho I, Cantalapiedra-Navarrete C, Liébanas G, Castillo P (2023) A blind-identification test on *Criconema annuliferum* (de Man, 1921) Micoletzky, 1925 species complex corroborate the hyper-cryptic species diversity using integrative taxonomy. *Plants* 12(5): 1044. <https://doi.org/10.3390/plants12051044>
- Archidona-Yuste A, Clavero-Camacho I, Ruiz-Cuenca AN, Cantalapiedra-Navarrete C, Liebanas G, Castillo P, Palomares-Rius JE (2024) The more we search, the more we find: Discovering and expanding the biodiversity in the ring nematode genus *Xenocriconemella* De Grisse and Loof, 1965 (Nematoda, Criconematidae). *Zoological Letters* 10(1): 8. <https://doi.org/10.1186/s40851-024-00230-3>

Barsi L, Fanelli E, De Luca F (2017) A new record of *Xiphinema dentatum* Sturhan, 1978 and description of *X. paradentatum* sp. n. (Nematoda, Dorylaimida) from Serbia. *Nematology* 19(8): 925–949. <https://doi.org/10.1163/15685411-00003098>

Bello A, Boag B, Thopham PB, Ibáñez J (1986) Geographical distribution of *Xenocriconemella macrodora* (Nematoda, Criconematidae). *Nematologia Mediterranea* 14: 223–229.

Cai R, Archidona-Yuste A, Cantalapiedra-Navarrete C, Palomares-Rius JE, Castillo P (2020) New evidence of cryptic speciation in the family Longidoridae (Nematoda, Dorylaimida). *Journal of Zoological Systematics and Evolutionary Research* 58(4): 869–899. <https://doi.org/10.1111/jzs.12393>

Cantalapiedra-Navarrete C, Navas-Cortés JA, Liébanas G, Vovlas N, Subbotin SA, Palomares-Rius JE, Castillo P (2013) Comparative molecular and morphological characterisations in the nematode genus *Rotylenchus*: *Rotylenchus paravitis* n. sp., an example of cryptic speciation. *Zoologischer Anzeiger* 252(2): 246–268. <https://doi.org/10.1016/j.jcz.2012.08.002>

Clavero-Camacho I, Palomares-Rius JE, Cantalapiedra-Navarrete C, León-Ropero G, Martín-Barbarroja J, Archidona-Yuste A, Castillo P (2021) Integrative taxonomy reveals hidden cryptic diversity within Pin nematodes of the genus *Paratylenchus* (Nematoda, Tylenchulidae). *Plants* 10(7): 1454. <https://doi.org/10.3390/plants10071454>

Coolen W (1979) Methods for the extraction of *Meloidogyne* spp. and other nematodes from roots and soil. In: Lamberti F, Taylor CE (Eds) *Root-knot nematodes (Meloidogyne species); systematics, biology and control*. Academic Press, New York, USA, 317–329.

Cordero MA, Robbins RT, Szalanski AL (2012) Taxonomic and molecular identification of *Bakernema*, *Criconema*, *Hemicriconemoides*, *Ogma* and *Xenocriconemella* species (Nematoda, Criconematidae). *Journal of Nematology* 44: 427–446.

Darriba D, Taboada GL, Doallo R, Posada D (2012) jModelTest 2: More models, new heuristics and parallel computing. *Nature Methods* 9(8): 772–772. <https://doi.org/10.1038/nmeth.2109>

Dayrat B (2005) Towards integrative taxonomy. *Biological Journal of the Linnean Society*. *Linnean Society of London* 85(3): 407–415. <https://doi.org/10.1111/j.1095-8312.2005.00503.x>

De Grisse AT (1969) Redescription ou modifications de quelques techniques utilisées dans l'étude de nématodes phytoparasitaires. *Mededelingen Rijksfaculteit Landbouwwetenschappen Gent* 34: 315–359.

De Grisse A, Loof PAA (1965) Revision of the genus *Criconemoides* (Nematoda). *Mededelingen van de Landbouwhogeschool en der opzoekingsstations van den Staat te Gent* 30: 577–603.

De Ley P, Felix MA, Frisse L, Nadler S, Sternberg P, Thomas WK (1999) Molecular and morphological characterisation of two reproductively isolated species with mirror-image anatomy (Nematoda, Cephalobidae). *Nematology* 1(6): 591–612. <https://doi.org/10.1163/156854199508559>

Decraemer W, Archidona-Yuste A, Clavero-Camacho I, Vovlas A, Cantalapiedra-Navarrete C, Ruiz-Cuenca AN, Castillo P, Palomares-Rius JE (2024) Unravelling cryptic diversity in the *Paratrichodorus allius*-group species complex to resolve eight new species of the genus and new insights on the molecular phylogeny (Nematoda, Trichodoridae). *Zoological Journal of the Linnean Society* zlad194. <https://doi.org/10.1093/zoolinnean/zlad194>

Derycke S, Remerie T, Vierstraete A, Backeljau T, Vanfleteren J, Vincx M, Moens T (2005) Mitochondrial DNA variation and cryptic speciation within the free-living marine nematode *Pellioiditis marina*. *Marine Ecology Progress Series* 300: 91–103. <https://doi.org/10.3354/meps300091>

Escuer M, Lara MP, Bello A (1999) Distribution of the Criconematidae in Peninsular Spain and Balearic Islands. *International Journal of Nematology* 9: 47–67.

Etongwe C, Singh R, Bert W, Subbotin S (2020) Molecular characterisation of some plant-parasitic nematodes (Nematoda, Tylenchida) from Belgium. *Russian Journal of Nematology* 28: 1–28. <https://doi.org/10.24411/0869-6918-2020-10001>

Fišer C, Koselj K (2022) Coexisting cryptic species as a model system in integrative taxonomy. In: Monro AK, Mayo SJ (Eds) *Cryptic Species: Morphological Stasis, Circumscription, and Hidden Diversity*. Cambridge University Press, Cambridge, 169–196. <https://doi.org/10.1017/9781009070553.007>

Gómez-Barcina A, Castillo P, González-País MA (1989) Nematodos fitoparásitos de la subfamilia Criconematinae Taylor, 1936 en la Sierra de Cazorla. *Revista Iberica de Parasitologia* 49: 241–255.

Gutiérrez-Gutiérrez C, Palomares-Rius JE, Cantalapiedra-Navarrete C, Landa BB, Esmenaud D, Castillo P (2010) Molecular analysis and comparative morphology to resolve a complex of cryptic *Xiphinema* species. *Zoologica Scripta* 39(5): 483–498. <https://doi.org/10.1111/j.1463-6409.2010.00437.x>

Hall TA (1999) BioEdit: A user-friendly biological sequence alignment editor and analysis program for windows 95/98/NT. *Nucleic Acids Symposium Series* 41: 95–98.

Hamilton CA, Hendrixson BE, Brewer MS, Bond JE (2014) An evaluation of sampling effects on multiple DNA barcoding methods leads to an integrative approach for delimiting species: A case study of the North American tarantula genus *Aphonopelma* (Araneae, Mygalomorphae, Theraphosidae). *Molecular Phylogenetics and Evolution* 71: 79–93. <https://doi.org/10.1016/j.ympev.2013.11.007>

Holterman M, van der Wurff A, van den Elsen S, van Megen H, Bongers T, Holovachov O, Bakker J, Helder J (2006) Phylum-wide analysis of SSU rDNA reveals deep phylogenetic relationships among nematodes and accelerated evolution toward crown clades. *Molecular Biology and Evolution* 23(9): 1792–1800. <https://doi.org/10.1093/molbev/msl044>

Hu M, Chilton NB, Zhu X, Gasser RB (2002) Single-strand conformation polymorphism-based analysis of mitochondrial cytochrome c oxidase subunit 1 reveals significant substructuring in hookworm populations. *Electrophoresis* 23(1): 27–34. [https://doi.org/10.1002/1522-2683\(200201\)23:1<27::AID-ELPS27>3.0.CO;2-7](https://doi.org/10.1002/1522-2683(200201)23:1<27::AID-ELPS27>3.0.CO;2-7)

Katoh K, Rozewicki J, Yamada KD (2019) MAFFT online service: multiple sequence alignment, interactive sequence choice and visualization. *Briefings in bioinformatics* 20: 1160–1166. <https://doi.org/10.1093/bib/bbx108>

Lê S, Josse J, Husson F (2008) FactoMineR: An r package for multivariate analysis. *Journal of Statistical Software* 25(1): 1–18. <https://doi.org/10.18637/jss.v025.i01>

Legendre P, Legendre L (2012) *Numerical Ecology*. 3<sup>rd</sup> edn. Elsevier, Amsterdam, The Netherlands, 990 pp.

Masters BC, Fan V, Ross HA (2011) Species Delimitation - a Genius plugin for the exploration of species boundaries. *Molecular Ecology Resources* 11(1): 154–157. <https://doi.org/10.1111/j.1755-0998.2010.02896.x>

Montgomery DC, Peck EA, Vining GG (2012) Introduction to linear regression analysis. John Wiley & Sons, Hoboken, New Jersey, 821 pp.

Myers N, Mittermeier RA, Mittermeier CG, da Fonseca GAB, Kent J (2000) Biodiversity hotspots for conservation priorities. *Nature* 403(6772): 853–858. <https://doi.org/10.1038/35002501>

Nguyen HT, Nguyen TD, Le TML, Trinh QP, Bert W (2022) Remarks on phylogeny and molecular variations of criconematid species (Nematoda, Criconematidae) with case studies from Vietnam. *Scientific Reports* 12(1): 14832. <https://doi.org/10.1038/s41598-022-18004-2>

Peraza-Padilla W, Aráuz-Badilla J, Cantalapiedra-Navarrete C, Palomares-Rius JE, Archidona-Yuste A, Castillo P (2024) A new ring nematode, *Xenocriconemella costaricense* sp. nov., (Nematoda, Criconematidae) from Costa Rica. *Journal of Helminthology* 98: e39. <https://doi.org/10.1017/S0022149X24000294>

Powers TO, Harris TS, Higgins RS, Mullin PG, Powers KS (2021) Nematode biodiversity assessments need vouchered databases: A BOLD reference library for plant-parasitic nematodes in the superfamily Criconematoidea. *Genome* 64: 232–241. <https://doi.org/10.1139/gen-2019-0196>

Proudlove G, Wood PJ (2003) The blind leading the blind: Cryptic subterranean species and DNA taxonomy. *Trends in Ecology & Evolution* 18(6): 272–273. [https://doi.org/10.1016/S0169-5347\(03\)00095-8](https://doi.org/10.1016/S0169-5347(03)00095-8)

R Core Team (2022) A language and environment for statistical computing. R Foundation for Statistical Computing, Vienna, Austria. <https://www.R-project.org/>

Rambaut A (2018) Rambaut A (2018) FigTree v1.4.4, A graphical viewer of phylogenetic trees. <http://tree.bio.ed.ac.uk/software/figtree/>

Ronquist F, Huelsenbeck JP (2003) MrBayes 3: Bayesian phylogenetic inference under mixed models. *Bioinformatics* 19(12): 1572–1574. <https://doi.org/10.1093/bioinformatics/btg180>

Rosenberg NA (2007) Statistical tests for taxonomic distinctiveness from observations of monophyly. *Evolution; International Journal of Organic Evolution* 61(2): 317–323. <https://doi.org/10.1111/j.1558-5646.2007.00023.x>

Ross HA, Murugan S, Li WL (2008) Testing the reliability of genetic methods of species identification via simulation. *Systematic Biology* 57(2): 216–230. <https://doi.org/10.1080/10635150802032990>

Seinhorst JW (1966) Killing nematodes for taxonomic study with hot F.A. 4:1. *Nematologica* 12(1): 178–178a. <https://doi.org/10.1163/187529266X00239>

Subbotin SA, Vierstraete A, De Ley P, Rowe J, Waeyenberge L, Moens M, Vanfleteren JR (2001) Phylogenetic relationships within the cyst-forming nematodes (Nematoda, Heteroderidae) based on analysis of sequences from the ITS regions of ribosomal DNA. *Molecular Phylogenetics and Evolution* 21(1): 1–16. <https://doi.org/10.1006/mpev.2001.0998>

Subbotin SA, Vovlas N, Crozzoli R, Sturhan D, Lamberti F, Moens M, Baldwin JG (2005) Phylogeny of *Criconematina* Siddiqi, 1980 (Nematoda, Tylenchida) based on morphology and D2-D3 expansion segments of the 28S-rRNA gene sequences with application of a secondary structure model. *Nematology* 7(6): 927–944. <https://doi.org/10.1163/156854105776186307>

Tan G, Muffato M, Ledergerber C, Herrero J, Goldman N, Gil M, Dessimoz C (2015) Current methods for automated filtering of multiple sequence alignments frequently worsen single-gene phylogenetic inference. *Systematic Biology* 64(5): 778–791. <https://doi.org/10.1093/sysbio/syv033>

Taylor AL (1936) The genera and species of the Criconematinae, a sub-family of the Anguillulinidae (Nematoda). *Transactions of the American Microscopical Society* 55(4): 391–421. <https://doi.org/10.2307/3222522>

Zuur AF, Ieno EN, Elphick CS (2010) A protocol for data exploration to avoid common statistical problems. *Methods in Ecology and Evolution* 1(1): 3–14. <https://doi.org/10.1111/j.2041-210X.2009.00001.x>